



Lamb Waves in a Fluid Saturated Incompressible Porous Plate Bordered with Layers of Inviscid Liquid

Rajneesh Kumar[†] and B. S. Hundal^{‡,1}

[†]Department of Mathematics, Kurukshetra University
Kurukshetra, Haryana, India

[‡]Department of Mathematics, S.R. Government College for Women
Amritsar, Punjab, India
e-mail : hundal_bs@yahoo.co.in

Abstract : The propagation of Lamb waves in a fluid saturated porous plate, consisting of a microscopically incompressible solid skeleton containing microscopically incompressible liquid and bordered with layers of inviscid liquid or half-spaces of inviscid liquid on both sides is investigated. The frequency equations for the plate in closed form and isolated mathematical conditions for symmetric and skew-symmetric wave modes in completely separate terms are derived. The results for empty porous incompressible isotropic elastic plate have been obtained as the particular cases. The special cases, such as short wavelength waves and the leaky Lamb waves are also obtained and discussed. Results at various steps are compared with the corresponding results of classical theory and finally the variations of phase velocity, attenuation coefficient with wave number and displacement amplitudes with distance from the boundary of the plate is presented graphically and discussed.

Keywords : incompressible porous medium; volume fractions; symmetric waves; skew-symmetric waves; frequency equation; phase velocity; wave number; attenuation coefficient.

2010 Mathematics Subject Classification : 74F10.

¹Corresponding author.

1 Introduction

Most of the modern engineering structures are generally made up of multi-phase porous continuum and the classical theory, which represents a fluid saturated porous medium as a single phase material, is inadequate to represent the mechanical behavior of such materials especially when the pores are filled with liquid. In this case the solid and liquid phases have the different motions. Due to these different motions, the different material properties and the complicated geometry of pore structure, the mechanical behavior of a fluid saturated porous medium becomes more difficult. So the researchers from time to time have tried to overcome this difficulty and a considerable work is available in the literature. For more detail and for the historical review on the subject of multiphase continuum mechanics, the reader is referred to the work of Boer and Ehlers [1] or Boer [2].

Based on the work of von Terzaghi [3, 4], Biot [5] proposed a general theory of three-dimensional deformations of fluid saturated porous solids. Then the wave propagation and the dynamic extensions were done by Biot [6–8]. Using his theory, Biot [9] studied the bending of a poro-elastic plate and on the basis of Biot's model, Taber [10] and Theodorakopoulos and Beskos [11] presented a general theory of poro-elastic flexural plates under quasi-static and dynamic conditions respectively. Biot theory is based on the assumption of compressible constituents and till recently, some of his results have been taken as standard references and the basis for subsequent analysis in acoustic, geophysics and other such fields. Although Biot's model was broadly accepted and applied, it has some shortcomings because it originated from experience, lacking strong mechanic foundation.

The theory of waves in plates was originally developed by Horace Lamb [12] and these waves are frequently referred to as Lamb waves. These are the waves generated in plates with free boundaries and with an infinite number of modes for symmetric and skew symmetric displacements within the plates. Wu and Zhu [13, 14] presented an analytical technique to assess the effect of viscous fluid loading on the propagation properties of Lamb waves in fluid loaded solids. But all this work is based on the theory where the plate is considered to be made up of single phase material. Based on the Fillunger model [15] (which is further based on the concept of volume fractions combined with surface porosity coefficients), Bowen [16], Boer and Ehlers [17, 18], Ehlers [19] developed and used another interesting theory in which all the constituents of a porous medium are assumed to be incompressible. There are reasonable grounds for the assumption that the constituents of many fluid saturated porous media are incompressible. Take, for example, the compositions of soil, the solid constituents are incompressible and liquid constituents which are generally water or oils are also incompressible. Moreover in an empty porous solid as a case of classical theory the change in volume is due to the change in porosity during the propagation of a longitudinal wave. The assumption of incompressible constituents does not only meet the properties appearing in many branches of engineering practice, but it also avoids the introduction of many complicated material parameters as considered in the Biot theory. So this model meets the requirements of further scientific developments. Based on this theory Boer et

al. [20], Liu and Boer [21], Yan et al. [22] and Svanadze [23] have studied the various problems of wave propagation in fluid saturated incompressible porous media. Kumar and Hundal [24] have discussed the corresponding Lamb waves in a fluid-saturated incompressible porous plate.

In the present paper we have discussed the analysis of Lamb type wave propagation in an infinite fluid saturated incompressible elastic plate bordered on both sides with layers or half-spaces of inviscid liquid. The implicit frequency equations connecting the phase velocity with wave number and other physical parameters are derived. The various cases as the propagation of leaky Rayleigh and Lamb type waves in the context of fluid saturated incompressible porous plate are also considered. The theoretical results obtained for symmetric and skew-symmetric modes of wave propagation have been verified numerically for a particular model and are discussed.

2 Formulation of the Problem and Its Solution

Consider an infinite fluid saturated incompressible porous elastic rectangular plate of thickness $2d$. The plate is bordered on top and bottom with infinitely long homogeneous inviscid liquid layers each of thickness h . If $h \rightarrow \infty$, then the problem becomes the case of leaky Lamb type waves in a fluid saturated incompressible porous plate. The coordinate system is selected with x, y -plane coinciding with the middle surface of the plate, x -axis along the length and z -axis normal to it along the thickness (Fig. 1). The surfaces $z = \pm d$ are subjected to different boundary conditions. Following Boer and Ehlers [18, 20] the equations governing the deformation of an incompressible porous medium saturated with non-viscous fluid in the absence of body forces are

$$\nabla \cdot (\eta^S \dot{\mathbf{u}}_S + \eta^F \dot{\mathbf{u}}_F) = 0, \quad (2.1)$$

$$(\lambda^S + \mu^S) \nabla (\nabla \cdot \mathbf{u}_S) + \mu^S \nabla^2 \mathbf{u}_S - \eta^S \nabla p - \rho^S \ddot{\mathbf{u}}_S + S_v (\dot{\mathbf{u}}_F - \dot{\mathbf{u}}_S) = \mathbf{0}, \quad (2.2)$$

$$\eta^F \nabla p + \rho^F \ddot{\mathbf{u}}_F + S_v (\dot{\mathbf{u}}_F - \dot{\mathbf{u}}_S) = \mathbf{0}, \quad (2.3)$$

$$\mathbf{T}_E^S = 2\mu^S \mathbf{E}_S + \lambda^S (\mathbf{E}_S \cdot \mathbf{I}) \mathbf{I}, \quad (2.4)$$

$$\mathbf{E}_S = \frac{1}{2} (\text{grad } \mathbf{u}_S + \text{grad}^T \mathbf{u}_S), \quad (2.5)$$

where \mathbf{u}_i , $\dot{\mathbf{u}}_i$ and $\ddot{\mathbf{u}}_i$ ($i = F, S$) denote the displacements, velocities and accelerations of solid and fluid phases respectively and p is the effective pore pressure of the incompressible pore fluid. ρ^S and ρ^F are the densities of the solid and fluid phases respectively. \mathbf{T}_E^S is the stress in the solid phase and \mathbf{E}_S is the linearized Lagrangian strain tensor. λ^S and μ^S are the macroscopic Lamé's parameters of the porous solid and η^S, η^F are the volume fractions satisfying

$$\eta^S + \eta^F = 1. \quad (2.6)$$

In the case of isotropic permeability, the tensor \mathbf{S}_V describing the coupled interaction between the solid and fluid is given by Boer and Ehlers [18, 20] as

$$\mathbf{S}_V = \frac{(\eta^F)^2 \gamma^{FR}}{K^F} \mathbf{I} = S_V \mathbf{I}, \quad (2.7)$$

where γ^{FR} is the effective specific weight of the fluid and K^F is the Darcy's permeability coefficient of the porous medium. Equations governing the motion of a liquid are given by Ewing et al. [25] as

$$\lambda^L \nabla (\nabla \mathbf{u}^L) = \rho^L \frac{\partial^2 \mathbf{u}^L}{\partial t^2}, \quad (2.8)$$

$$\tau_{mn}^L = \lambda^L \nabla \mathbf{u}^L \delta_{mn}, \quad m, n = 1, 2, 3. \quad (2.9)$$

In these two equations \mathbf{u}^L is the displacement vector, λ^L is the bulk modulus of the liquid, ρ^L is its density and τ_{mn}^L are the components of the stress in the liquid.

For further considerations, it is convenient to introduce, in equations (2.1)-(2.9), the dimensionless quantities defined as:

$$\begin{aligned} x' = \frac{\omega'}{c_1} x, z' = \frac{\omega'}{c_1} z, t' = \omega' t, \mathbf{u}'^S = \left(\frac{\lambda^S + 2\mu^S}{E} \frac{\omega'}{c_1} \right) \mathbf{u}^S, \mathbf{u}'^F = \left(\frac{\lambda^S + 2\mu^S}{E} \frac{\omega'}{c_1} \right) \mathbf{u}^F, \\ p' = \frac{p}{E}, \mathbf{T}'^S = \frac{\mathbf{T}^S}{E}, \tau'_{mn} = \frac{\tau_{mn}^L}{E}, \mathbf{u}'^L = \left(\frac{\lambda^S + 2\mu^S}{E} \frac{\omega'}{c_1} \right) \mathbf{u}^L. \end{aligned} \quad (2.10)$$

In these relations E is the Young's modulus of the solid phase, ω' is the characteristic frequency of the medium and c_1 is the velocity of a longitudinal wave propagating in a fluid saturated incompressible porous medium and is given by [20] as

$$c_1 = \sqrt{\frac{(\eta^F)^2 (\lambda^S + 2\mu^S)}{(\eta^F)^2 \rho^S + (\eta^S)^2 \rho^F}}. \quad (2.11)$$

If the pore liquid is absent or gas is filled in the pores, then ρ^F is very small as compare to ρ^S and can be neglected. So the relation (2.11) reduces to

$$c_0 = \sqrt{\frac{\lambda^S + 2\mu^S}{\rho^S}}. \quad (2.12)$$

This gives the velocity of the longitudinal wave propagating in an incompressible empty porous solid, where the change in volume is due to the change in porosity and is a well-known result of the classical theory of elasticity [25]. In an incompressible non-porous solid medium $\eta^F \rightarrow 0$, then (2.11) yields $c_1 = 0$ and is physically acceptable as a longitudinal wave cannot propagate in an incompressible medium.

The equations (2.1)-(2.5), (2.8) and (2.9) with the help of (2.10) reduce to the dimensionless form and after slashing the dashes, the dimensionless displacement vectors \mathbf{u}^i ($i = S, F, L$) are expressed in terms of potential φ^i and ψ^i as:

$$\mathbf{u}^i = \text{grad}\varphi^i - \text{curl}\psi^i. \quad (2.13)$$

We take $x-z$ plane as the plane of incidence and assume all the physical quantities to depend upon x, z and time t . Also the inviscid liquid does not support shear motion so the shear modulus of liquid vanishes and hence the potential ψ^L also vanish. So the equations (2.1)-(2.3) and (2.8) with the help of (2.13) yields the following equations

$$\frac{\partial^2 \varphi^S}{\partial x^2} + \frac{\partial^2 \varphi^S}{\partial z^2} - \eta^S \rho - \delta_1^2 \frac{\partial^2 \varphi^S}{\partial t^2} - \frac{\delta_2}{(\eta^F)^2} \frac{\partial \varphi^S}{\partial t} = 0, \quad (2.14)$$

$$\delta^2 \left(\frac{\partial^2 \psi^S}{\partial x^2} + \frac{\partial^2 \psi^S}{\partial z^2} \right) - \delta_1^2 \frac{\partial^2 \psi^S}{\partial t^2} + \delta_2 \left(\frac{\partial \psi^F}{\partial t} - \frac{\partial \psi^S}{\partial t} \right) = 0, \quad (2.15)$$

$$\varphi^F = -\frac{\eta^S}{\eta^F} \varphi^S, \quad (2.16)$$

$$\eta^F \rho + \frac{\rho^F}{\rho^S} \delta_1^2 \frac{\partial^2 \varphi^F}{\partial t^2} + \delta_2 \left(\frac{\partial \varphi^F}{\partial t} - \frac{\partial \varphi^S}{\partial t} \right) = 0, \quad (2.17)$$

$$\frac{\rho^F}{\rho^S} \delta_1^2 \frac{\partial^2 \psi^F}{\partial t^2} + \delta_2 \left(\frac{\partial \psi^F}{\partial t} - \frac{\partial \psi^S}{\partial t} \right) = 0, \quad (2.18)$$

$$\frac{\partial^2 \varphi^{L_j}}{\partial x^2} + \frac{\partial^2 \varphi^{L_j}}{\partial z^2} = \delta_3^2 \frac{\partial^2 \varphi^{L_j}}{\partial t^2}, \quad (2.19)$$

where

$$\delta = \frac{\beta_0}{c_0}, \delta_1 = \frac{c_1}{c_0}, \beta_0 = \sqrt{\frac{\mu^S}{\rho^S}}, \delta_2 = \frac{S_V c_1^2}{\omega' \rho^S c_0^2}, \delta_3 = \frac{c_1}{\alpha_L}, \alpha_L = \sqrt{\frac{\lambda^L}{\rho^L}} \quad (2.20)$$

and $j = 1, 2$ stands for top and bottom liquid layers respectively.

The solutions of equations (2.14)-(2.19) for the harmonic waves are given by

$$\varphi^S = (P_1 \cos \xi_1 z + P_2 \sin \xi_1 z) e^{i(kx \sin \theta - \omega t)}, \quad (2.21)$$

$$\varphi^F = -\frac{\eta^S}{\eta^F} (P_1 \cos \xi_1 z + P_2 \sin \xi_1 z) e^{i(kx \sin \theta - \omega t)}, \quad (2.22)$$

$$\psi^S = (P_3 \cos \xi_2 z + P_4 \sin \xi_2 z) e^{i(kx \sin \theta - \omega t)}, \quad (2.23)$$

$$\psi^F = \frac{i}{i + P\omega} (P_3 \cos \xi_2 z + P_4 \sin \xi_2 z) e^{i(kx \sin \theta - \omega t)}, \quad (2.24)$$

$$\varphi^{L_1} = P_5 \sin \{ \xi_3 (z - (d + h)) \} e^{i(kx \sin \theta - \omega t)} d < z < d + h, \quad (2.25)$$

$$\varphi^{L2} = -P_6 \sin \{ \xi_3 (z - (d + h)) \} e^{i(kx \sin \theta - \omega t)} (d + h) < z < -d, \quad (2.26)$$

where

$$\xi_1^2 = k^2 \left(c^2 + i \frac{Qc}{k} - S_1^2 \right), \quad (2.27)$$

$$\xi_2^2 = k^2 \left[\left\{ \delta_1^2 + \frac{\delta_2 P (1 + iP\omega)}{(1 + P^2\omega^2)} \right\} \left(\frac{c}{\delta} \right)^2 - S_1^2 \right], \quad (2.28)$$

$$\xi_3^2 = k^2 (\delta_3^2 c^2 - S_1^2), \quad (2.29)$$

$$P = \frac{\delta_1^2 \rho^F}{\delta_2 \rho^S}, Q = \frac{\delta_2}{(\eta^F)^2}, S_1 = \sin \theta \quad (2.30)$$

and P_m , ($m = 1, 2, \dots, 6$) are the arbitrary constants. The phase velocity $\frac{\omega}{k}$ of the waves is denoted by c and θ is the angle of inclination of wave normal with the axis of symmetry. With the help of (2.4), (2.5), (2.9) and (2.13) the expressions for displacements, stresses and pore-pressure are obtained as

$$u^S = \{ ikS_1 (P_1 \cos \xi_1 z + P_2 \sin \xi_1 z) + \xi_2 (-P_3 \sin \xi_2 z + P_4 \cos \xi_2 z) \} e^{i(kx \sin \theta - \omega t)}, \quad (2.31)$$

$$w^S = \{ \xi_1 (-P_1 \sin \xi_1 z + P_2 \cos \xi_1 z) - ikS_1 (P_3 \cos \xi_2 z + P_4 \sin \xi_2 z) \} e^{i(kx \sin \theta - \omega t)}, \quad (2.32)$$

$$u^F = \left\{ -k \frac{\eta^S}{\eta^F} (P_1 \cos \xi_1 z + P_2 \sin \xi_1 z) + \frac{i\xi_2}{(1 + iP\omega)} (-P_3 \sin \xi_2 z + P_4 \cos \xi_2 z) \right\} \times e^{i(kx \sin \theta - \omega t)}, \quad (2.33)$$

$$w^F = - \left\{ \frac{\eta^S}{\eta^F} \xi_1 (-P_1 \sin \xi_1 z + P_2 \cos \xi_1 z) + \frac{kS_1}{(1 + iP\omega)} (P_3 \cos \xi_2 z + P_4 \sin \xi_2 z) \right\} \times e^{i(kx \sin \theta - \omega t)}, \quad (2.34)$$

$$\tau_{zz} = \left\{ \left(2\delta^2 k^2 S_1^2 - \omega^2 - \frac{i\omega \delta_2}{(\eta^F)^2} \right) (P_1 \cos \xi_1 z + P_2 \sin \xi_1 z) - 2\delta^2 \xi_2 ikS_1 (-P_3 \sin \xi_2 z + P_4 \cos \xi_2 z) \right\} e^{i(kx \sin \theta - \omega t)} \quad (2.35)$$

$$\tau_{xz} = \left[2\delta^2 ik\xi_1 S_1 (-P_1 \sin \xi_1 z + P_2 \cos \xi_1 z) + \left\{ 2\delta^2 k^2 S_1^2 - \delta_1^2 \omega^2 - \frac{\delta_2 P \omega^2}{(1 + P^2 \omega^2)} \right\} \times (P_3 \cos \xi_2 z + P_4 \cos \xi_2 z) \right] e^{i(kx \sin \theta - \omega t)} \quad (2.36)$$

$$p = -\frac{1}{(\eta^F)^2} \left(\frac{\eta^S \rho^F}{\rho^S} \omega^2 + i\delta_2 \omega \right) (P_1 \cos \xi_1 z + P_2 \sin \xi_1 z) e^{i(kx \sin \theta - i\omega t)}, \quad (2.37)$$

$$u_z^{L1} = \xi_3 P_5 \cos \{ \xi_3 (z - (d+h)) \} e^{i(kx \sin \theta - i\omega t)} d < z < d+h, \quad (2.38)$$

$$u_z^{L2} = -\xi_3 P_6 \cos \{ \xi_3 (z - (d+h)) \} e^{i(kx \sin \theta - i\omega t)}, -(d+h) < z < -d, \quad (2.39)$$

$$\tau_{zz}^{L1} = -\frac{\rho^L}{\rho^S} \delta_1^2 \omega^2 P_5 \sin \{ \xi_3 (z - (d+h)) \} e^{i(kx \sin \theta - i\omega t)} d < z < d+h, \quad (2.40)$$

$$\tau_{zz}^{L2} = \frac{\rho^L}{\rho^S} \delta_1^2 \omega^2 P_6 \sin \{ \xi_3 (z - (d+h)) \} e^{i(kx \sin \theta - i\omega t)} -(d+h) < z < -d. \quad (2.41)$$

3 Derivation of Frequency Equations

The boundary conditions at the solid – liquid interfaces $z = \pm d$ to be satisfied are

(i) The total normal stress of the plate should be equal to the pressure of the liquid. This implies that

$$\tau_{zz}^S - p = \tau_{zz}^{Lj}, j = 1, 2. \quad (3.1)$$

(ii) The shear stress in the fluid saturated incompressible poro-elastic plate must vanish, i.e.

$$\tau_{xz}^S = 0. \quad (3.2)$$

(iii) The normal component of the displacement of the solid should be equal to that of liquid. This leads to

$$u_z^S = u_z^{Lj}, j = 1, 2. \quad (3.3)$$

So using the above boundary conditions, we obtain six simultaneous equations for the unknowns P_m ($m = 1, 2, \dots, 6$). The condition, for their non trivial solution leads to a characteristic equation for the propagation modified Lamb waves in a fluid saturated incompressible porous plate bordered with layers of inviscid liquid or half-spaces of inviscid liquid on both sides. After some manipulations of the determinant, we get the following frequency equations for symmetric and skew-symmetric modes of wave propagation:

$$\frac{\tan \xi_2 d}{\tan \xi_1 d} + \frac{R_3 (R_2 \xi_3 - R_L k S_1 \tan \xi_2 d \tan \xi_3 h)}{R_4 (R_1 \xi_3 + R_L \xi_1 \tan \xi_1 d \tan \xi_3 h)} = 0, \quad (3.4)$$

$$\frac{\tan \xi_2 d}{\tan \xi_1 d} + \frac{R_4 (R_1 \xi_3 - R_L \xi_1 \cot \xi_1 d \tan \xi_3 h)}{R_3 (R_2 \xi_3 + R_L k S_1 \cot \xi_1 d \tan \xi_3 h)} = 0, \quad (3.5)$$

where

$$R_1 = 2\delta^2 k^2 S_1^2 - \left\{ 1 - \frac{\rho^F}{\rho^S} \frac{\eta^S \delta_1^2}{(\eta^F)^2} \right\} \omega^2, \quad (3.6)$$

$$R_2 = 2\delta^2 S_1 \xi_2 k, \quad (3.7)$$

$$R_3 = 2\xi_1 S_1 k, \quad (3.8)$$

$$R_4 = 2k^2 S_1^2 - \left\{ \delta_1^2 + \frac{\delta_2 P (1 + iP\omega)}{(1 + P^2\omega^2)} \right\} \left(\frac{\omega}{\delta} \right)^2, \quad (3.9)$$

and

$$R_L = \frac{\rho^L}{\rho^S} \delta_1^2 \omega^2. \quad (3.10)$$

Equations (3.4) and (3.5) are the frequency equations for symmetric and skew-symmetric modes of wave propagation in an infinite fluid saturated incompressible porous elastic solid rectangular plate bordered with layers of inviscid liquid or half-spaces of inviscid on both sides.

4 Some Special Cases

4.1 The Rayleigh–Lamb Frequency Equation for Fluid Saturated Incompressible Porous Plate Having Traction Free Boundaries

In the absence of liquid layers, equations (3.4) and (3.5), after some simplifications, reduce to

$$\frac{\tan \xi_2 d}{\tan \xi_1 d} + \left\{ \frac{4k^2 \delta^2 S_1^2 \xi_1 \xi_2}{R_1 (k^2 S_1^2 - \xi_2^2)} \right\}^{\pm 1} = 0, \quad (4.1)$$

Here the subscripts +1 and –1 refer to the symmetric and skew-symmetric waves. If the pore liquid is absent or gas is filled in the pores then ρ^F is very small as compare to ρ^S and can be neglected. So after some simplifications equation (4.1) takes the form

$$\frac{\tan \xi_2' d}{\tan \xi_1' d} + \left\{ \frac{4k^2 S_1^2 \xi_1' \xi_2'}{(k^2 S_1^2 - \xi_2'^2)^2} \right\}^{\pm 1} = 0. \quad (4.2)$$

Equations (4.2) are the Rayleigh-Lamb frequency equations for straight as well as crested waves propagating in an empty incompressible porous elastic plate. ξ_1' and ξ_2' can be obtained from (2.27) and (2.28) by taking P and Q to be zero. For $\theta = \frac{\pi}{2}$, equation (4.2) is a well known result of classical theory and is available in the standard texts, e.g., Graff [26].

4.2 Leaky Lamb Waves in a Fluid Saturated Incompressible Porous Plate

The dispersion relations for leaky Lamb waves, i.e. Lamb waves in a fluid saturated incompressible porous plate bordered with infinite half spaces of homogeneous liquid can be obtained just by letting $h \rightarrow \infty$ in equations (3.4) and (3.5)

so we have

$$\frac{\tan \xi_2 d}{\tan \xi_1 d} + \frac{R_3 (R_2 \xi_3 - i R_L k S_1 \tan \xi_2 d)}{R_4 (R_1 \xi_3 + i R_L \xi_1 \tan \xi_1 d)} = 0, \tag{4.3}$$

for symmetric mode of waves and

$$\frac{\tan \xi_2 d}{\tan \xi_1 d} + \frac{R_4 (R_1 \xi_3 - i R_L \xi_1 \cot \xi_1 d)}{R_3 (R_2 \xi_3 + i R_L k S_1 \cot \xi_1 d)} = 0, \tag{4.4}$$

for skew-symmetric modes of wave propagation.

4.3 Waves of Short Wave-Length

Some information on the asymptotic behavior is obtained by letting $k \rightarrow \infty$. In this case we replace ξ_1, ξ_2 and ξ_3 by another complex numbers $i\xi'_1, i\xi'_2$ and $i\xi'_3$ respectively. So for the waves of short wavelength, as $k \rightarrow \infty$, the frequency equations (3.4) and (3.5) for both symmetric and skew- symmetric cases reduce to

$$\frac{\frac{\rho^L}{\rho^S} \delta_1^2 c^2}{\sqrt{S_1^2 - \delta_L^2 c^2}} = \frac{4\delta^2 S_1^2 \sqrt{S_1^2 - c^2} \sqrt{S_1^2 - \left\{ \delta_1^2 + \frac{\delta_2 P(1+iP\omega)}{(1+P^2\omega^2)} \right\}} \left(\frac{c}{\delta}\right)^2 - \left[2\delta^2 S_1^2 - \left\{ 1 - \frac{\rho^F}{\rho^S} \frac{\eta^S \delta_1^2}{(\eta^F)^2} \right\} c^2 \right] \left[2S_1^2 - \left\{ \delta_1^2 + \frac{\delta_2 P(1+iP\omega)}{(1+P^2\omega^2)} \right\} \left(\frac{c}{\delta}\right)^2 \right]}{\left\{ \delta_1^2 + \frac{\delta_2 P(1+iP\omega)}{(1+P^2\omega^2)} \right\} \sqrt{S_1^2 - c^2}} \tag{4.5}$$

Equation (4.5) is the dispersion relation for leaky Rayleigh type waves propagating in an infinite fluid saturated incompressible porous half-space bordered with a half-space of a homogeneous inviscid liquid. Again in the absence of liquid layers ($\rho^L \rightarrow 0$), we have a traction free fluid saturated incompressible plate and in this case equation (4.5) for the waves of short wave length is simplified to

$$4S_1^2 \sqrt{S_1^2 - \left\{ \delta_1^2 + \frac{\delta_2 P(1+iP\omega)}{(1+P^2\omega^2)} \right\}} \left(\frac{c}{\delta}\right)^2 - \frac{\left[2S_1^2 - \left\{ \delta_1^2 + \frac{\delta_2 P(1+iP\omega)}{(1+P^2\omega^2)} \right\} \left(\frac{c}{\delta}\right)^2 \right] \left\{ 2S_1^2 - \left(1 - \frac{\eta^S \rho^F \delta_1^2}{(\eta^F)^2 \rho^S} \right) \left(\frac{c}{\delta}\right)^2 \right\}}{\sqrt{S_1^2 - c^2}} = 0. \tag{4.6}$$

The equation (4.6) governs the propagation of Rayleigh type surface waves at the free surface of a fluid saturated incompressible porous half-space. The vibrational energy is mainly propagates along the surface of the plate and the finite thickness plate appears as a semi-infinite media. Again if the pore liquid is absent or gas is filled in the pores and $\theta = \frac{\pi}{2}$, then after some simplifications equation (4.6) becomes

$$4\sqrt{\left(1 - \frac{c^2}{\delta^2}\right)} (1 - c^2) = \left(2 - \frac{c^2}{\delta^2}\right)^2. \tag{4.7}$$

If the dimensionless quantities are converted in to the corresponding physical quantities, then the equation (4.7) yields

$$4\sqrt{\left(1 - \frac{c^2}{c_0^2}\right) \left(1 - \frac{c^2}{\beta_0^2}\right)} = \left(2 - \frac{c^2}{\beta_0^2}\right)^2. \quad (4.8)$$

The above equation corresponds to the Rayleigh wave propagating along the free surface of a half-space of an empty incompressible porous solid and is a well-known result of classical theory.

Thus we see that if the pore liquid is absent, then both P and Q given by (2.30) will be zero and we obtain the results, which are in good agreement with the classical theory. So besides changing the velocity of propagation, the presence of fluid in the pores of an incompressible porous solid also give arise the imaginary terms in the equations (2.27) and (2.28), highlighting the fact that the presence of fluid in the pores of a fluid saturated incompressible porous elastic solid makes the waves more dissipative.

5 Numerical Results and Discussion

With the view of illustrating the theoretical results obtained in the preceding sections, this section deals with the numerical results for the dispersion relations. Equations (3.4) and (3.5) determine the phase velocity c of the symmetric and skew-symmetric waves as a function of wave number k and various physical parameters in complex form, showing that the waves are attenuated in space. If we write

$$\frac{1}{c} = \frac{1}{v} + i\frac{q}{\omega} \quad (5.1)$$

so that the wave-number $k = K_1 + iq$, where $K_1 = \frac{\omega}{v}$, v and q are real numbers. This shows that v is the propagation speed, K_1 is the real wave number and q is the attenuation coefficient of the waves. Also for a particular model the values of the various physical parameters are taken as $E = 2.01 \times 10^7 \text{N/m}^2$, $\nu = 0.20$, $\eta^S = 0.67$, $\eta^F = 0.33$, $\rho^S = 2.01 \times 10^3 \text{Kg/m}^3$, $\rho^F = 1.0 \times 10^3 \text{Kg/m}^3$, $k^F = 0.01 \text{ m/s}$, $\gamma^{\text{FR}} = 1.0 \times 10^4 \text{ N/m}^3$. The liquid taken for the purpose of numerical calculations is water, where the velocity of sound is given by $c_L = 1.5 \times 10^3 \text{ m/s}$. The thickness of the plate is taken to be 6 whereas the thickness of each of the bordering layer is taken to be 1. The angles of inclination of the wave normal with the axis of symmetry have been taken between 0 and $\frac{\pi}{2}$ for numerical calculations. As $\tan(n\pi + \alpha) = \tan \alpha$, so for the given values of wave number, the equations (3.4) and (3.5) are solved for three different values of n and for three values of θ by using the method of successive approximation. The sequence of iteration is made to converge after sampling it over about 150 sample values in order to achieve the desired level of accuracy (five decimal places here). The variations of numerically computed phase velocity v and attenuation coefficient q with real wave-number K_1 are shown graphically in Figs. 2–5 for wave normal inclination

$\theta = 30^\circ$, 60° and 90° with the axis of symmetry.

From Fig. 2 it is observed that the phase velocity for lowest (fundamental) symmetric mode is almost constant for $\theta = 30^\circ$, where as it is observed to increase for $\theta = 60^\circ$ and decrease for $\theta = 90^\circ$ from some small values at the vanishing wave-number and ultimately become closer to leaky Rayleigh wave velocity at higher values of the wave-number. The phase velocity for fundamental skew-symmetric mode is non-dispersive and remains near to leaky Rayleigh wave velocity for all directions of wave propagation. But the phase velocity of higher (optical) modes of wave propagation for both symmetric and skew symmetric cases attains quite large values at the vanishing wave number, which sharply slashes down to become steady and asymptotic to the leaky Rayleigh wave velocity with increasing wave number. The significant fall at the vanishing wave number is caused by the damping effect of the liquid layers on both sides of the plate and also the viscous damping caused by internal friction from the interaction mechanism between the skeleton and pore liquid present in the pores of the fluid saturated incompressible elastic porous solid. The asymptotic closeness of various mode of propagation is due to the fact that in the limiting case when the wave number is large the problem reduces to the leaky Rayleigh type waves in a fluid saturated incompressible porous half-space. The finite thickness plate and the bordering layers behave like semi-infinite media. Study is given for three values of n and for three values of inclination of the wave normal with the axis of symmetry and it is evident that the phase velocity increases with both these quantities.

The surface waves propagate with complex wave number and hence the phase velocity. Consequently, the surface waves propagate with attenuation due to the radiation of energy into the medium. It is observed that the presence of fluid in the pores makes them even more attenuated. The Figs. 4 and 5, depict the variation of attenuation coefficients versus wave number for symmetric and skew – symmetric modes for $n = 4$. For the symmetric waves, the attenuation coefficient remains small and constant for $\theta = 30^\circ$. For $\theta = 60^\circ$ and 90° it increases monotonically from zero in the interval $0 \leq K_1 \leq 0.52$ to acquire its maximum values 0.0597 and 0.018 for $\theta = 60^\circ$ and $\theta = 90^\circ$ respectively at $K_1 = 0.52$ then decreases in $0.52 \leq K_1 \leq 1.5$. Thereafter, the attenuation coefficient remains constant in all directions of wave propagation. In case of skew-symmetric modes, the behavior of attenuation coefficient is different from the above case. It is almost zero for $\theta = 60^\circ$, increases uniformly from zero for other two values of θ and again slashes down to zero with increasing wave number. For $\theta = 30^\circ$ it attains a maximum value of 0.0264 at $K_1 = 0.52$, whereas the maximum value for $\theta = 90^\circ$ is 0.0959 at $K_1 = 2.02$.

The variations of various amplitudes of displacements with distance from the free surfaces of the plate are presented in Figs. 6 – 13 for symmetric and skew-symmetric waves. The variations are discussed in the region $-3 \leq z \leq 3$, because for the present discussion; the value of d is taken to be 6. For symmetric waves, starting from some value, the horizontal displacement amplitudes vary in such a way that the variation curves are symmetrical about y -axis Fig. 6. As θ varies the curves change their shapes from concave upward to convex upward. The

magnitude of displacement amplitude also varies with θ and for $\theta = 90^\circ$ it has maximum value at the middle surface of the plate. The vertical displacement amplitudes are zero at the middle surface of the plate and the variation curves are symmetrical in the opposite quadrants (Fig. 8). Among the three considered values of θ , the vertical displacement amplitude is maximum for $\theta = 60^\circ$ whereas it has minimum value for $\theta = 90^\circ$. Except for the change in their magnitudes, the variation curves of the horizontal displacement amplitudes for skew-symmetric waves follow the pattern of the vertical displacement curves for symmetric waves Fig. 10. The variation curves of the vertical displacement amplitudes for skew-symmetric waves (Fig. 12) are also symmetrical about y-axis, but at the middle surface of the plate, the magnitudes of displacement amplitudes decreases with θ and the curves are concave downward. As a result of the incompressibility constraint, the motion of the fluid phase is in opposite direction to that of solid phase and except for their magnitude, the variation curves for fluid phase, Figs. 7, 9, 11 and 13, follow the reverse pattern as followed by the corresponding curves for the solid phase.

6 Conclusion

Based on the general incompressible porous media theories, a mathematical study is presented to discuss the wave propagation in a fluid saturated incompressible porous elastic plate bordered with layers of inviscid liquid on both sides. The material of plate is modeled as a two-phase system with two incompressible constituents (porous solid and inviscid fluid), where the general field equations are directly adopted according to the work of Boer and Ehlers [18, 20]. The assumption of two incompressible constituents does not only meets the properties appearing in the many porous media models, but it also avoids the introduction of many complicated material parameters as considered in the Biot theory. At the short wavelength limit the problem reduces to leaky Rayleigh waves in a fluid saturated incompressible plate and the finite thickness plate and the bordering layers behave like infinite media. It has been analyzed that the presence of pore liquid has a significant effect on the wave propagation. The variations of phase velocity, attenuation coefficient with wave number and the amplitude of various displacements with distance from the free surfaces are discussed. It is observed that the waves for fundamental mode are dispersion less and phase velocity for other modes become asymptotic to the leaky Rayleigh wave velocity for the larger value of the wave number. The results obtained are in good agreement with the classical theories. It is noticed that the inclination of the wave normal with the axis of symmetry also affects the dispersion behavior of the surface waves.

References

- [1] R. de Boer, W. Ehlers, A historical review of the formulation of porous media theories, *Acta Mechanica* 74 (1988) 1–8.

- [2] R. de Boer, *Theory of Porous Media*, Springer-Verlag, New York, 2000.
- [3] K. von Terzaghi, Die Berechnung der Durchlässigkeit des Tones aus dem Verlauf der hydromechanischen Spannungserscheinungen, *Sitzungsber. Akad. Wiss. (Wien)*, Math. Naturwiss. Kl., Abt. IIa 132 (1923) 125–138.
- [4] K. von Terzaghi, *Erdbaumechanik auf Bodenphysikalischer Grundlage*, Franz Deuticke, Leipzig and Vienna. (1925) p. 399.
- [5] M.A. Biot, General theory of three dimensional consolidation, *J. Appl. Phys.* 12 (2) (1941) 155–161.
- [6] M.A. Biot, Theory of propagation of elastic waves in a Fluid-saturated porous solid-I, *J. Acoust. Soc. Am.* 28 (1956a) 168–178.
- [7] M.A. Biot, Theory of propagation of elastic waves in a Fluid-saturated porous solid -II, *J. Acoust. Soc. Am.* 28 (1956b) 179–191.
- [8] M.A. Biot, Mechanics of deformation and acoustic propagation in porous media, *J. Appl. Phys.* 33 (4) (1962) 1482–1498.
- [9] M.A. Biot, Theory of buckling of a porous slab and its thermo-elastic analogy, *J. Appl. Mech. ASME* 31 (1964) 194–198.
- [10] Taber, L. A.: A theory for transverse deflection of poroelastic plates, *J. Appl. Mech. ASME* 59 (1992) 628–634.
- [11] D.D. Theodorakopoulos, D.E. Beskos. Flexural vibrations of fissured poroelastic plates, *Arch. Appl. Mech.* 63 (6) (1993) 413–423.
- [12] H. Lamb, On waves in elastic plates, *Proc. Roy. Soc. London, Ser. A* 93 (1917) 114–128.
- [13] J. Wu, Z. Zhu, The propagation of Lamb waves in a plate bordered with layers of a liquid, *J. Acoust. Soc. Am.* 91 (1992) 861–867.
- [14] Z. Zhu, J. Wu, The propagation of Lamb waves in a plate bordered with a viscous liquid, *J. Acoust. Soc. Am.* 98 (1995) 1057–1064.
- [15] P. Fillunger, *Der Auftrieb in Talsperren*. Osterr. Wochenschrift für den öffentl. Baudienst, Franz Deuticke, Wien, 1913.
- [16] R.M. Bowen, Incompressible Porous Media Models by use of the Theory of Mixtures, *Int. J. Engg. Sci.* 18 (1980) 1129–1148.
- [17] R. de Boer, W. Ehlers, The development of the concept of effective stress, *Acta Mechanica* 83 (1990) 77–92.
- [18] R. de Boer, W. Ehlers, Uplift, Friction and capillarity-three fundamental effects for liquid-saturated porous solids, *Int. J. Solid Structures* 26 (1990) 43–57.
- [19] W. Ehlers, Compressible, incompressible and hybrid two-phase models in porous theories, *ASME; AMD* 158 (1993) 25–38.

- [20] R. de Boer, W. Ehlers, Z. Liu, One-dimensional transient wave propagation in a fluid-saturated incompressible porous media, *Arch. App. Mech.* 63 (1993) 59–72.
- [21] Z. Liu, R. de Boer, Dispersion and attenuation of surface waves in a fluid-saturated porous medium, *Transp. Porous Media* 29 (1997) 207–223.
- [22] B. Yan, Z. Liu, X. Zhang, Finite element analysis of wave propagation in a fluid-saturated porous media, *Applied Mathematics and Mechanics* 20 (1999) 1331–1341.
- [23] M. Svanadze, R. de Boer, W. Ehlers, Z. Liu, On the representation of solutions in the theory of fluid-saturated incompressible porous media, *Q. J. Mech. Appl. Math.* 58 (4) (2005) 551–562.
- [24] R. Kumar, B.S. Hundal, Circular crested lamb waves in a fluid-saturated incompressible porous plate, *Multidiscipline Modeling in Materials and Structures* 4 (2008) 369–384.
- [25] W.M. Ewing, W.S. Jardetzky, F. Press, *Elastic Waves in Layered Media*, McGraw – Hill Book Co., 1957.
- [26] K.F. Graff, *Wave Motion in Elastic Solids*, Dower Publications, New York, 1991.

(Received 4 March 2011)

(Accepted 19 June 2012)

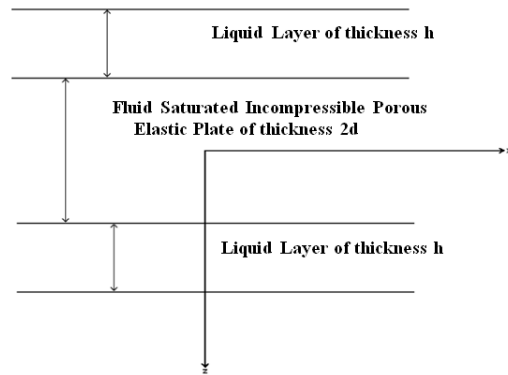


Fig. 1: Geometry of the Investigated Problem.

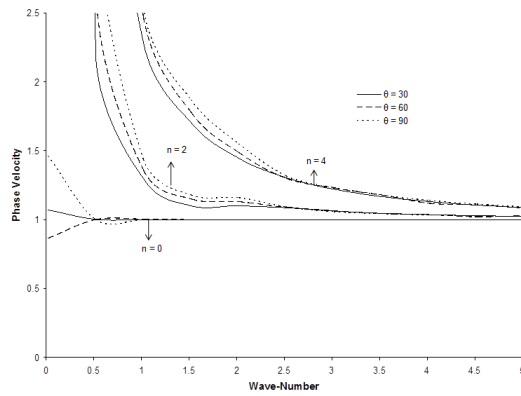


Fig. 2: Variation of Phase Velocity with Wave-Number and θ (for Symmetric Waves).

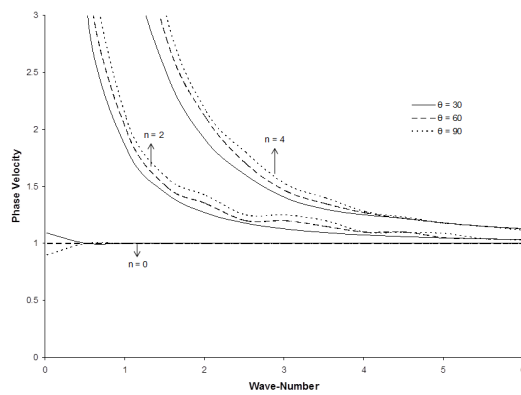


Fig. 3: Variation of Phase Velocity with Wave-Number and θ (for Skew-Symmetric Waves).

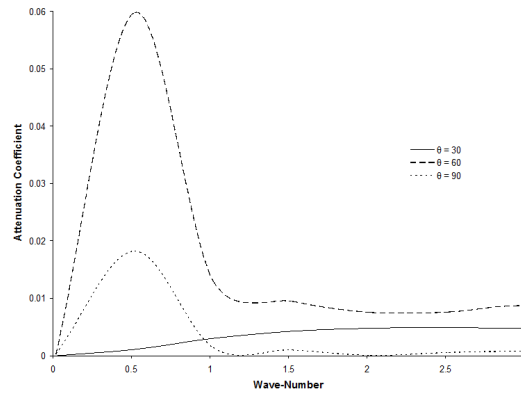


Fig. 4: Variations of Attenuation Coefficient with Wave-Number and θ (for Symmetric Waves).

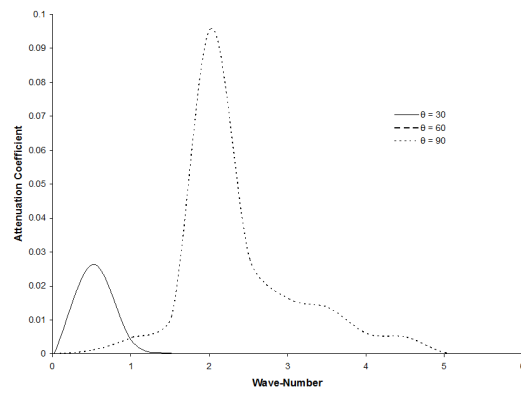


Fig. 5: Variations of Attenuation Coefficient with Wave-Number and θ (for Skew-Symmetric Waves).

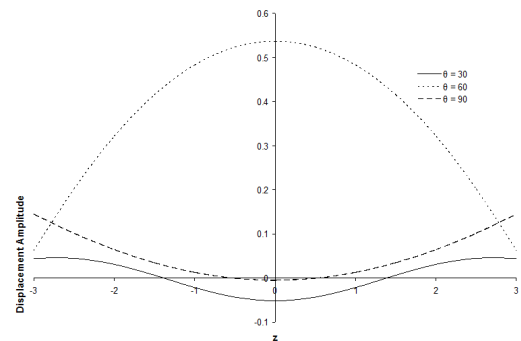


Fig. 6: Variation of Horizontal, Solid Displacement Amplitude with z and θ for Symmetric Waves.

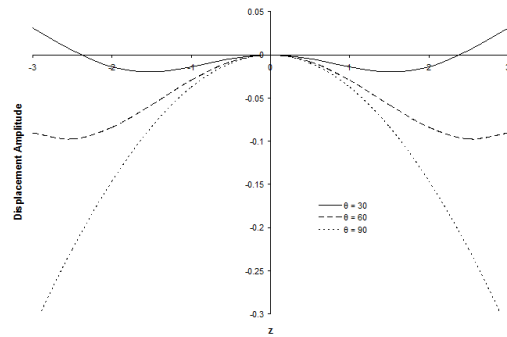


Fig. 7: Variation of Horizontal, Fluid Displacement Amplitude with z and θ for Symmetric Waves.

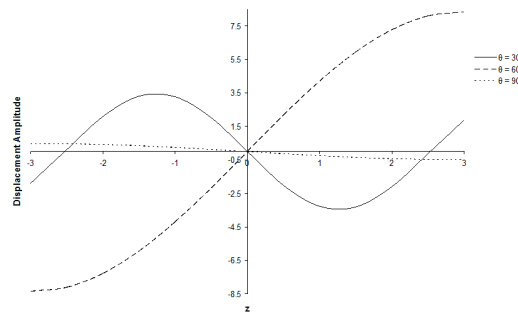


Fig. 8: Variation of Vertical, Solid Displacement Amplitude with z and θ for Symmetric Waves.

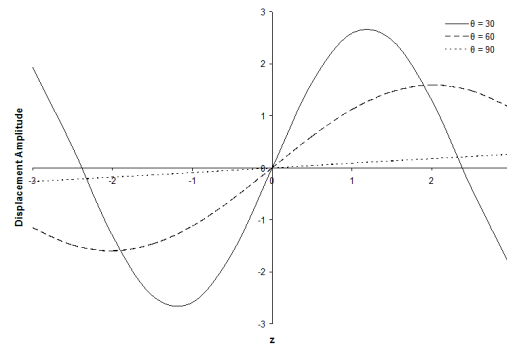


Fig. 9: Variation of Vertical, Fluid Displacement Amplitude with z and θ for Symmetric Waves.

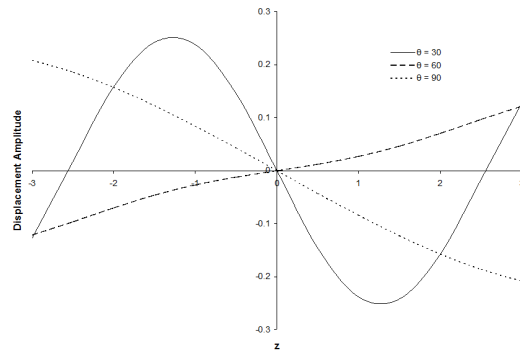


Fig. 10: Variation of Horizontal, Solid Displacement Amplitude with z and θ for Skew-Symmetric Waves.

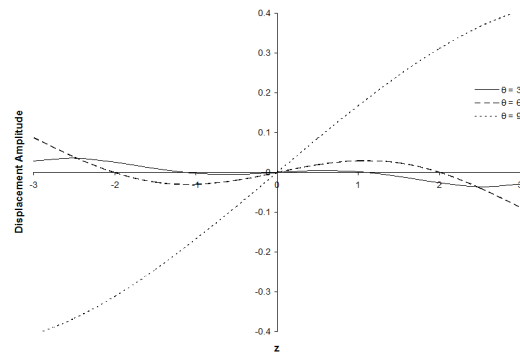


Fig. 11: Variation of Horizontal, Fluid Displacement Amplitude with z and θ for Skew-Symmetric Waves.

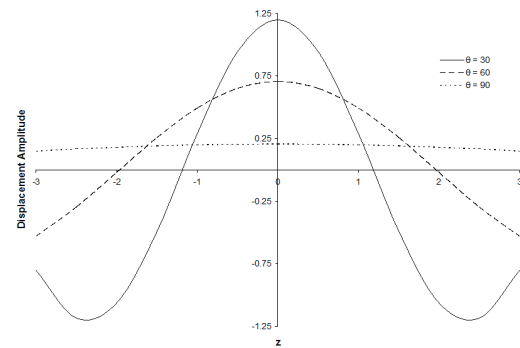


Fig. 12: Variation of Vertical, Solid Displacement Amplitude with z and θ for Skew-Symmetric Waves.

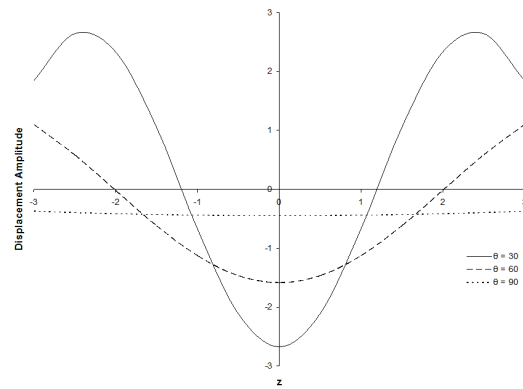


Fig. 13: Variation of Vertical, Fluid Displacement Amplitude with z and θ for Skew-Symmetric Waves.